PIECEWISE SMOOTH IMAGE COMPRESSION USING NORMAL DISPLACEMENT MAPS

W. Van Aerschot
Computer Science Dept., K.U.Leuven
Celestijnenlaan 200 A,
B3001 Heverlee - Belgium,
Ward.VanAerschot@cs.kuleuven.be

M. Jansen
Department of Math., K.U.Leuven
Celestijnenlaan 200 B,
B3001 Heverlee - Belgium,
Maarten.Jansen@wis.kuleuven.be

A. Bultheel
Computer Science Dept., K.U.Leuven
Celestijnenlaan 200 A,
B3001 Heverlee - Belgium,
Adhemar.Bultheel@cs.kuleuven.be

Abstract

This paper applies the idea of normal mesh techniques, utilized in CG rendering applications of smooth manifolds in 3d space, to piecewise smooth functions defined on the plane. The nonsmoothness of these functions is located along a smoothly varying curve in the domain. The nonlinear nature of the proposed method allows to deal with the 'regularity' of the curve. The smooth curve is approximated by a polyline existing of triangle edges of the adaptively created nested triangulations. The proposed method can be used in transform coders generating sparse representations of piecewise smooth colored images. We state a full compression algorithm to encode images where all information is located in one smooth contour.

Index terms —- normal displacement maps, wavelets, image compression

1 INTRODUCTION

Today's object scanning hardware allows to capture high density point clouds producing tons of data which can be post-processed for very high resolution representation of the original object. Many applications let users interacts with these models. Such interactivity requests for efficient storage and rendering techniques. Short response times are being mimicked by producing outputs which gradually increase in detail. The detail information is often stored in displacement maps, i.e. maps consisting of vector data relative to the previous approximating mesh, allowing to represent the data at several levels of detail. Interacting with a coarse approximation of the scanned object will be fast while more and more detail is added when processing power is available. When dealing with 'smooth' objects it is shown [2, 3, 5, 6] that the majority of the displacement vectors can be restricted to a direction normal to the approximating mesh. These normal displacement maps only contain scalar data.

Having a coarse base mesh that interpolates the given surface, normal displacement maps are created as follows: from each edge of the current mesh a ray is shot normal to the mesh from the midpoint until it pierces the (closed) surface. Only the distance from the edge midpoint to this piercing point has to be stored.

The idea of using normal mesh techniques in order to approximate piecewise smooth *functions* is quite new [4]. This in contrast with previously mentioned applications involving smooth surfaces homeomorphic to the sphere. In this paper we redefine some fundamental properties of the normal *transform* of [4]. We combine the transform with an appropriate modelling of the normal offsets to allow for an *entropy coder* and obtain a practical algorithm applicable in digital image transform coders.

The paper is outlined as follows. Section 2 explains which properties make normal meshes suitable for on the one hand sparsely representing smooth 3d surfaces and on the other hand sparsely representing piecewise smooth images. In Section 3 the proposed normal mesh algorithm is outlined. The efficient encoding of the wavelet coefficients (normal offsets) is done by a model based entropy coder and will be explained in Section 4. Section 5 compares the approximation rate of the proposed transform and the wavelet transform and shows rate-distortion curves of the proposed encoder compared to the JPEG2000 encoder.

2 PIECEWISE SMOOTH IMAGES

Images represented as functions on the plane can also be seen as surfaces in 3d space. Despite the similarities between surface and image compression we cannot take 'off the shelf' normal mesh encoders and apply them to the surface equivalents of a geometrical image. The first

major difference concerns the smoothness properties of the target surfaces. While surfaces in computer graphics are smooth, geometrical images on the other hand are non-smooth: the line discontinuities are the information carrying feature. A second major difference – and the actual reason for using a normal offset transform in an image compression algorithm– is the exploitation of normal approximation properties in order to compress. The reason for using normal offsets in surface rendering applications is that they contain almost all geometrical information [3]. Semi-regular meshes are sufficient to represent connection information so that little topological information is needed. Using scalar displacement maps instead of vector maps leads to a compression factor of three. In contrast, a continuous tone gray image is mostly given as a set of grey values on a fixed 2d regular grid and not as a collection of triple coordinates in R^3. The fundamental reason for using normal offsets in image processing is the edge locating property of the normal search direction. Irregular meshes have to be used to adapt the domain triangulation to avoid contour intersections.

3 THE ALGORITHM

We now give a specific implementation of each step the normal offset *transformation* scheme.

First, the location of new points are predicted by means of a subdivision rule on neighbouring mesh vertices. Although higher order subdivision can be applied we use a midpoint prediction rule. Let $\mathcal{E}_j$ be the set of edges of the interpolating mesh on resolution level j. The for each $e_{j,k} \in \mathcal{E}_j$, with k the positional index, a prediction point is calculated as $p^*_{j+1,2k+1} = (p_{j,k} + p_{j,k+1})/2$, with $p_{j,k}$ and $p_{j,k+1}$ the endpoints of $e_{j,k}$.

The correction step corrects the location of the prediction points by adding a vector in the direction normal to the coarse mesh to pinpoint a piercing point. Only the signed distance between prediction an piercing point is stored in the displacement map. Piercing point are located by travelling the normal ray starting from the prediction point until the difference between the z-value of the normal ray and the z-value of the surface changes sign. This definition of a piercing point can deal with discontinuous jumps in the surface during the search. When we constrain the ray to be normal to $e_{j,k}$ and to lie in a plane normal to the xy plane (the image domain), the piercing procedure creates proper parameterisations i.e. : $x_{j,k} \leq x_{j+1,2k+1} \leq x_{j,k+1}$. The piercing point $p_{j+1,2k+1}$ is inserted between $p_{j,k}$ and $p_{j,k+1}$ in order to form the sequence $\mathbf{p}_{j+1}$: The function above $e_{j,k}$ is gradually approximated by a polyline (a continuous curve composed of several line segments) through the sequence $\mathbf{p}_j = \left\{p_{j,0}, \ldots, p_{j,k} \ldots, p_{j,2^j+1}\right\}$.

Previous steps created piercing points that are to be inserted into the coarse mesh to form a higher resolution mesh. Each coarse triangle is split into 4 subtriangles. The subtriangles are formed from the parent triangles vertices and the piercing points corresponding with each triangle edge to form a conformal triangulation. The piercing points are connected to the end points of the edge they come from. In addition, for each adjacent triangle, they are connected to a piercing point from an other edge of the same triangle, or to the opposite vertex.

This yields four possible triangle splits. The choice is image dependent and is chosen by means of an error metric between the approximation and the surface. The two-bit topological codes have to be stored to allow reconstruction at the decoder side.

In the digital setting, next to normal offsets, also *vertical* offsets v have to be introduced to ensure perfect reconstruction. The latter offsets compensate for jumps that are present between almost every pixel.

4 COMPRESSION

This paper focuses on a special class of geometrical images. The class of Horizon images $\mathcal{H}$ existing of two constant colored regions separated by one smooth line discontinuity:

$$\mathcal{H} = \left\{f_\Omega(x,y)_{c(x)}\right\} \mid c(x) \in \mathcal{C}^2 \;\; \&$$
$$f_\Omega(x,y)_{c(x)} = \left\{ \begin{array}{ll} H & c(x) > y \\ 0 & c(x) \leq y \end{array} \right. , H \in \mathbf{R}$$

Next subsections derive probability density functions for both vertical and normal offsets. This will allow for an entropy coder to efficiently allocate codewords to the transform coefficients.

4.1 Model for the vertical offsets

The detail information or the high-frequency part of the input signal is gathered into vertical offsets, i.e. the difference between the value of the piercing point and the real function value. At regions where the underlying functions behave unpredictable, for instance in th presence of jumps (contours), noize or have a high curvature, those offsets tend to be big. According to [7] and confirmed by the experiments shown in Figure 1, the vertical offsets v, can be modeled by a two-parametric zero inflated geometrical distribution ZID(p, λ) (see [1] and references therein) given by:

$$v \sim f_V(v) = p\delta(v) + (1-p)\lambda/2(1-\lambda)^v.$$

The parameters p and λ can be obtained using a maximum-likelihood estimate (MLE) method.

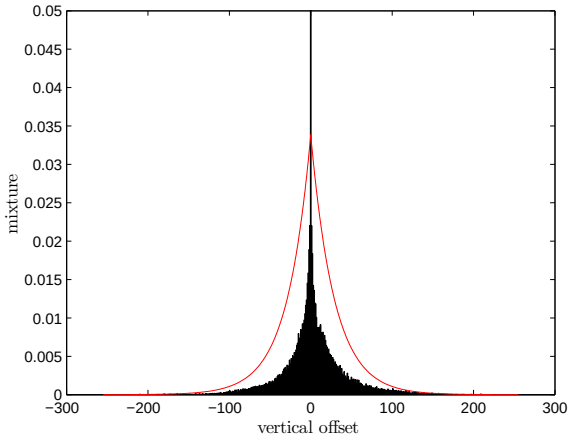

Figure 1. Histogram of the vertical offsets coming from a large test set of geometrical images. The figure suggests a zero inflated double geometrical distribution to model the statistics of the vertical offsets. The parameters produced by the MLE procedure are $p = 0.3955$ and $\lambda = 0.0339$.

4.2 Model for the normal offsets

Except for normal rays parallel to the z-axis, we can use the projection of the normal detail vector on the xy-plane to reconstruct the piercing point. This approach benefits that the number of possible projections is bounded by the length of the edge. The projections will further be called normal *indices*, and be denoted by i.

The normal indices can be encoded directly with codewords of $\lceil \log_2 L_{j,k} \rceil$ bits, with $L_{j,k}$ the number of pixels in the edge $e_{j,k}$ decaying like $O(2^{-j})$. This corresponds by assuming a uniform distribution.

We derive a more appropriate PMF associated with i for the class of Horizon images which allows an entropy encoder such as a Huffman encoder to lower the expected bitrate. Assume that a discontinuity is present between both edge points when $H \geq l$, (H the difference between the z-values of the edge end points, l the length of the edge in the domain) then the PDF is given by:

$$f(i) = \begin{array}{ll} 1/l, & i \in [-l/2, l/2] \\ 0, & \text{else} \end{array}$$

Assume that one of the endpoints of the edge is located at the discontinuity then for $H \geq l$

$$f(i) = \begin{cases} 1/2, & i = \pm l/2 \\ 0, & \text{else} \end{cases} .$$

Analogue for $H < l$. For the digital setting we have to introduce vertical offsets and obtain similar PMF models $f_i(i) = f_i(i|V_0 = v_0, V_1 = v_1) * f_{V_0}(v_0) * f_{V_1}(v_1)$, with v_0 and v_1 the vertical offsets at both endpoints of the edge, $f_X(x)$ the PMF (probability mass function) of x.

Which model should be applied will depend on wether a triangle edge is crossed by a contour, is flat, or lies with one of its endpoints at a singularity and on the slope of the edge. This can be predicted by an heuristic algorithm based on previous encoded data.

5 CONCLUSIONS AND RESULTS

This paper presents a nonlinear normal mesh based transform allowing sparse representations of smooth functions containing smooth line singularities. The transform adaptively decomposes the input image into a hierarchical triangle mesh representation having normal displacement maps. Combined with appropriate distribution models for the normal offset coefficients, the proposed transform can be used in a transform coder. Using a wavelet

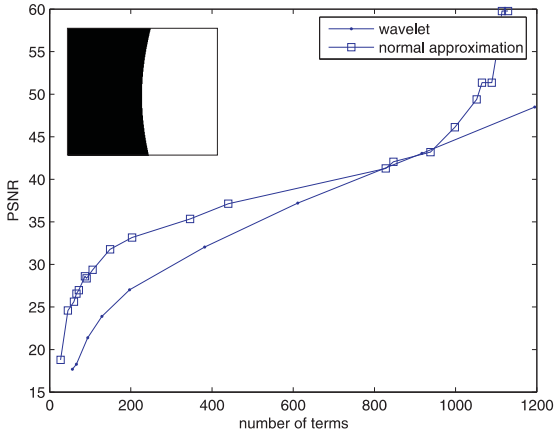

Figure 2. The approximation rate of a wavelet and a normal offset transform on an Horizon type image.

transform combined with a nonlinear thresholding step, the highest achievable n-term approximation rate equals $\sigma_{L_2} = O(n^{-\frac{1}{2}})$. In [4] it is proven that using their version of a normal offset based method achieves and n-term approximation rate equal to $\sigma_{L_2} = O(n^{-1})$.

We compare the approximation performance of both a nonlinear wavelet transform (the nonlinearity is introduced by the thresholding step) and the proposed normal offset transform of which both the transform as the n-terms selection is nonlinear. A 7-level wavelet decomposition was performed using the daubechies$7/9$ wavelet basis. The number of nonzero wavelet coefficients are counted after a hard thresholding step. For the normal offset transform the number of nonzero normal and vertical offsets are counted. The

results are given in Figure 2. When the region around the contour is the dominating factor for PSNR improvement, the rate at which the normal offset method approximates the image outperforms that of the wavelet based method. Wavelet approximated image typically show ringing artifacts around the contour.

Figure 3 compares our encoder with the JPEG2000 standard on a simple geometrical image. This preliminary result seems promising since the encoding can still be enhanced by including rate-distortion optimized quantizer on the vertical offsets.

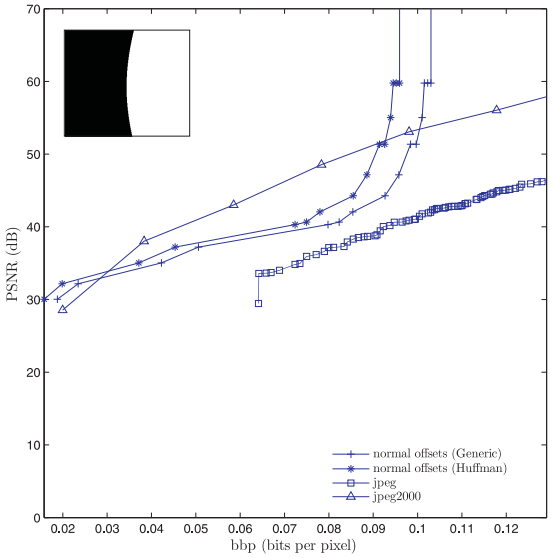

Figure 3. The rate distortion curve of a JPEG encoder and a JPEG2000 encoder together with the rate distortion curve of a normal offset encoder without using offset modeling (Generic) and a normal offset encoder using the proposed models as input for an Huffman entropy encoder (Huffman) is shown.

6 ACKNOWLEDGMENTS

The work is supported by the Fund for Scientific Research (FWO) project SMID: Stability of Multiscale Transforms on Irregular Data, grant #G.0431.05 and the Belgian Programme on Interuniversity Poles of Attraction, initiated by the Belgian Federal Science Policy Office and by the Center Of Excellence on Optimization in Engineering of the K.U.Leuven.

References

[1] D. Agarwal, A. Gelfand, and S. Citron-Pousty. Zero-inflated models with application to spatial count data. *Environmental and Ecological Statistics*, 9(4):pp. 341–355, December 2002.

[2] P. S. A.Khodakovsky and W. Sweldens. Progressive geometry compression. In K. Akeley, editor, *Siggraph 2000, Computer Graphics Proceedings*, pages 271–278. ACM Press / ACM SIGGRAPH / Addison Wesley Longman, 2000.

[3] I. Guskov, K. Vidimče, W. Sweldens, and P. Schröder. Normal meshes. In *SIGGRAPH 2000 Conference Proceedings*, 2000.

[4] M. Jansen, R. Baraniuk, and S. Lavu. Multiscale approximation of piecewise smooth two-dimensional functions using normal triangulated meshes. *Appl. Comp. Harm. Anal.*, 2005.

[5] A. Khodakovsky and I. Guskov. Compression of normal meshes. In *Geometric Modeling for Scientific Visualization*, pages 189–207. Springer Verlag, 2003.

[6] H. C. S. Lavu and R. Baraniuk. Geometry compression of normal meshes using rate-distortion algorithms. In *SGP '03: Proceedings of the 2003 Eurographics/ACM SIGGRAPH symposium on Geometry processing*, pages 52–61, Aire-la-Ville, Switzerland, Switzerland, 2003. Eurographics Association.

[7] E. Simoncelli. Modeling the joint statistics of images in the wavelet domain. In M. A. Unser, A. Aldroubi, and L. A. F., editors, *Wavelet Applications in Signal and Image Processing VII*, volume 3813 of *SPIE Proceedings*, pages 206–214, July 1999.